

The MINER ν A Data Acquisition System and Infrastructure

G. N. Perdue^{P,*}, L. Bagby^c, B. Baldin^c, C. Gingu^c, J. Olsen^c, P. Rubinov^c,
 E. C. Schulte^{h,1}, R. Bradford^{P,2}, W. K. Brooks^k, D. A. M. Caicedo^a,
 C. M. Castromonte^a, J. Chvojka^P, H. da Motta^a, I. Dankoⁿ, J. Devan^b,
 B. Eberlyⁿ, J. Felixⁱ, L. Fields^f, G. A. Fiorentini^a, A. M. Gago^g, R. Gran^o,
 D. A. Harris^c, K. Hurtado^{a,j}, H. Lee^P, E. Maher^e, S. Manly^P,
 C. M. Marshall^P, K. S. McFarland^P, A. Mislivec^P, J. Mousseau^m,
 B. Osmanov^m, J. Osta^c, V. Paoloneⁿ, R. D. Ransome^h, H. Ray^m,
 D. W. Schmitz^c, C. Simon^l, C. J. Solano Salinas^j, B. G. Tice^h, T. Walton^d,
 J. Wolcott^P, D. Zhang^b, B. P. Ziemer^l

^a*Centro Brasileiro de Pesquisas Físicas, Rua Dr. Xavier Sigaud 150, Urca, Rio de Janeiro, RJ, 22290-180, Brazil*

^b*Department of Physics, College of William & Mary, Williamsburg, Virginia 23187, USA*

^c*Fermi National Accelerator Laboratory, Batavia, Illinois 60510, USA*

^d*Hampton University, Dept. of Physics, Hampton, VA 23668, USA*

^e*Massachusetts College of Liberal Arts, 375 Church Street, North Adams, MA 01247, USA*

^f*Northwestern University, Evanston, Illinois 60208, USA*

^g*Sección Física, Departamento de Ciencias, Pontificia Universidad Católica del Perú, Apartado 1761, Lima, Perú*

^h*Rutgers, The State University of New Jersey, Piscataway, New Jersey 08854, USA*

ⁱ*Universidad de Guanajuato. Lascaraín de Retana No. 5. Col. Centro. Guanajuato 37150, Guanajuato. México*

^j*Universidad Nacional de Ingeniería, Tupac Amaru Avenue 210, Lima, Perú*

^k*Departamento de Física, Universidad Técnica Federico Santa María, Avda. España 1680 Casilla 110-V Valparaíso, Chile*

^l*Department of Physics and Astronomy, University of California – Irvine, Irvine, California 92697-4575, USA*

^m*Department of Physics, University of Florida, Gainesville, FL 32611, USA*

ⁿ*Department of Physics and Astronomy, University of Pittsburgh, Pittsburgh, Pennsylvania 15260, USA*

*Corresponding Author

Email address: perdue@fnal.gov (G. N. Perdue)

¹Present Address: Temple University, Philadelphia, PA 19122-6099, USA

²Present Address: Argonne National Laboratory, 9700 S. Cass Avenue, Lemont, IL 60439, USA

^oDepartment of Physics, University of Minnesota – Duluth, Duluth, Minnesota 55812, USA

^pUniversity of Rochester, Rochester, New York 14610 USA

Abstract

MINER ν A (Main INjector ExpeRiment ν -A) is a new few-GeV neutrino cross section experiment that began taking data in the FNAL NuMI (Fermi National Accelerator Laboratory Neutrinos at the Main Injector) beam-line in March of 2010. MINER ν A employs a fine-grained scintillator detector capable of complete kinematic characterization of neutrino interactions. This paper describes the MINER ν A data acquisition system (DAQ) including the read-out electronics, software, and computing architecture.

Keywords: DAQ, Data Acquisition, Minerva, Neutrinos

1. Introduction

MINER ν A (Main INjector ExpeRiment ν -A) is a low-to-medium energy neutrino-nucleus scattering experiment at FNAL (Fermi National Accelerator Laboratory). It utilizes the high-intensity NuMI (Neutrinos at the Main Injector) beamline and sits in the MINOS (Main Injector Neutrino Oscillation Search) Near Detector Hall, directly in front of the MINOS Near Detector and 105 meters below grade. MINER ν A does not extend far enough in the beam direction to range out muons with momentum over about 2 GeV/c, so the MINOS Near Detector is directly employed as a muon spectrometer. The references contain more detailed information on the physics program and general details of MINER ν A¹, MINOS², and the NuMI beam³.

This document discusses the MINER ν A data acquisition system (DAQ) in two steps. First, the custom electronics are described, followed by a description of the DAQ software and computing architecture.

The initial specifications for the DAQ readout system asked for a readout rate of ~ 100 kB/s with a duty factor defined by one ~ 10 microsecond beam spill every 2.2 seconds⁴. Fortunately, those specifications were surpassed as our initial estimate for required data throughput was low by about a factor of five.

20 **2. Overview of the Readout Scheme in MINER ν A**

21 The DAQ, slow controls (SC), and near-online monitoring (“nearline”)
22 systems are built around MINER ν A-specific readout electronics. MINER ν A
23 utilizes plastic scintillator as its fundamental detector technology. Light
24 is delivered via wavelength shifting fiber to Hamamatsu R7600 64-channel
25 multi-anode photomultiplier tubes (PMTs)⁵. A small number of single-anode
26 PMTs are also mounted for a “Veto Wall” detector that sits in front of the
27 main MINER ν A detector.

28 Each PMT is read out by a Front End Board (FEB)⁶ mounting six
29 Application-Specific Integrated Circuit (ASIC) chips (TriP-t chips)⁷ that dig-
30 itize and store charge using pipeline ADCs. Input charges from the PMT an-
31 odes are divided into high, medium, and low gain channels using a capacitive
32 divider to increase the dynamic range. The high gain is 1.25 fC/ADC, the
33 medium is 4 fC/ADC, and the low is 15.6 fC/ADC. The FEBs generate the
34 high voltage for most of the PMTs using an on-board Cockroft-Walton (CW)
35 generator. The control circuitry resides on the FEB, while the CW chain it-
36 self resides on the base, with appropriate taps for each dynode. A small
37 number of the PMTs are single-anode and use resistor-base technology for
38 voltage control. These PMTs are used to read out the Veto Wall and employ
39 a separate voltage control system discussed below. All FEB operations are
40 controlled by a Spartan 3E Field-Programmable Gate Array (FPGA) chip.
41 The FPGAs decode timing signals received over the unshielded twisted pair
42 (UTP) cables, sequence the TriP-t chips and decode and respond appropri-
43 ately to communication frames received over the data link. The FPGA also
44 controls the CW and other aspects of FEB operation. For data collection,
45 the boards are daisy-chained together (into “chains”) using standard UTP
46 ethernet networking cables with a custom protocol and Low Voltage Differ-
47 ential Signaling (LVDS). Of the four pairs in the cable, one is dedicated to
48 timing, including clock and encoded signals, one is dedicated for data, one
49 is used to indicate the sync-lock status of the data Serializer/Deserializer
50 (SERDES) and one for a test pulse.

51 The readout chain is connected at both ends to a custom VME mod-
52 ule called the Chain ReadOut Controller (CROC)⁸. A CROC supports four
53 Front End (FE) channels, each serving one chain of up to fifteen FEBs,
54 though no chain is longer than ten FEBs in MINER ν A. Each of the four
55 CROC channels contains a 6 kB dual-port memory for storing messages
56 (called “frames”) from the FEBs. The CROCs in turn receive timing and

57 trigger commands from another custom VME module, the CROC Interface
58 Module (CRIM)⁸, each of which distributes timing to up to four CROCs.
59 MINER ν A uses two VME crates, each containing a CAEN V2718 crate con-
60 troller⁹, two CRIMs, and roughly a half-dozen CROCs. There is no hit-based
61 trigger but rather a timing-based integration gate synchronized to the FNAL
62 Main Injector (MI) timing signals. Finally, the CRIMs receive information
63 from the timing system of the MINOS experiment (used for event match-
64 ing) and the state of the MI via the MINER ν A Timing Module (MvTM)¹⁰.
65 The MvTM does not have a VME interface, but uses the VME crate for
66 power. The start time in MINOS detector timing coordinates is logged as
67 a 28-bit number in the DAQ Header bank data. See Table 1 for a com-
68 plete module and card accounting. Only one MvTM is required to service all
69 timing needs. Each individual crate is readout by a computer (PC) mount-
70 ing a CAEN A2818 PCI card¹¹ that communicates with the crate controller
71 module via optical cable.

Era	VME Crates	CROCs	FEBs	Total Channels
Fall 2009	2	8	272	17,408
Spring 2010	2	14	491	31,424
Summer 2010 +	2	15	509	32,576

Table 1: MINER ν A read-out hardware installations.

72 An integration gate on the FEBs is opened synchronously with the de-
73 livery of neutrino beam spills. Beam spills delivered by the MI are approx-
74 imately 10 microseconds long, and are delivered every 2.2 or 2.06 seconds,
75 depending on the MI operating mode. Our readout gate opens 500 nanosec-
76 onds before the arrival of the spill and remains open 5.5 microseconds af-
77 ter the end. During normal data-taking, one additional calibration gate is
78 recorded between neutrino spills, either a random sampling of the detector
79 noise (a pedestal gate) or in coincidence with LEDs flashing the PMTs (a
80 “light-injection” gate). Pedestals are used to establish baseline readout lev-
81 els and light-injection to monitor gain drifts in the PMTs by studying the
82 photo-statistics of the LED signals.

83 At the end of the gate, the readout system runs a software loop over all
84 of the FEBs and collects data in the form of device “frames” (well-defined
85 and formatted byte data with attached headers) one at a time for the state
86 of the high-voltage, hit timing, and finally the hit blocks themselves. Each

87 frame is passed through a chain to a CROC FE channel where it is stored
88 briefly before being passed to a readout computer for archival and monitoring
89 processes.

90 Readout of the electronics is done in pairs of nested loops. Requests for
91 data are sent to the first FEB on each FE channel before looping back to
92 retrieve the data from the CROC memory. Then the next set of FEBs are
93 handled in another dual loop over FE channels, etc. This allows the DAQ
94 computers to communicate with the next CROC while the previous one is
95 fetching data from the FEBs on one of its readout chains.

96 In normal data-taking MINER ν A reads out in a “zero suppression” mode.
97 In this mode, the DAQ first reads the discriminator frame data for each
98 board and stores frames that contain hits above the discriminator threshold
99 (about 70 fC). It then loops over those boards and reads the FPGA registers
100 and all time-stamped ADC hit block frames. The FEBs are configured to
101 enable readout of up to eight ADC blocks: seven time-stamped hits and
102 one “un-timed” hit at the end of the integration gate. The un-timed hit
103 carries no discriminator timing information and contains all the integrated
104 charge between the last timed hit and the end of the gate. The FPGA
105 registers contain configuration data, high-voltage read-back, and the local
106 “gate time stamp” - the time the gate was opened for integration in the local
107 FEB counter time coordinates. Boards without hits above threshold are not
108 read out in this loop and neither are un-time-stamped ADC frames (charge
109 collected below threshold and stored until the end of the integration gate).
110 All seven available time-stamped hits are read out. During construction
111 and early low-energy configuration running, a configuration with five time-
112 stamped hits and one “un-timed” end-of-gate hit was used. See Table 2 for
113 a listing of the sizes of each data type.

114 Despite using more than 32,000 active channels in MINER ν A, the quan-
115 tity of data per neutrino spill is not large due to low interaction cross-sections.
116 With a 2.2 second MI cycle and 35×10^{12} protons on target per spill, roughly
117 1 MB per spill for the entire detector in zero-suppression mode running in
118 the NuMI low-energy configuration is collected, where the most frequent neu-
119 trino energy is ~ 3 GeV. About half of those data are beam spill data and
120 half are calibration data.

121 Readout time for a single frame is approximately 500 microseconds. Most
122 of that time is in message preparation and in setting up a block transfer; for
123 our data the readout speeds per frame are largely insensitive to the size of the
124 frame. Physics gate readouts typically require 1200 frames on average, while

Frame Type	Size (bytes)	Comments
FPGA Programming	66	Spartan 3E control registers.
ADC	444	Hit data.
Discriminator	16 + 40 per TriP-t per hit	Time stamps for each hit.
TriP Programming	652 (read) 758 (write)	TriP-t internal registers.
DAQ Header	48	Not a true “frame.” → End of gate marker.

Table 2: Frame sizes per FEB for MINER ν A data objects. The FPGA programming frames track configuration details and provide data on the high voltage, gate initiation time, and some useful error-checking bits. The TriP-t chips were originally designed for the D0 experiment¹² and so carried timing data that is not usable by MINER ν A. These data were trimmed in the packing algorithm for more efficient use of space. This reduced storage bloat, but did not meaningfully impact speed. Only discriminator frames are of variable size. The TriP-t programming frames are not read or written to during data acquisition. They are only accessed during configuration stages by the slow controls.

125 calibration gate readouts require 1600 (channel occupancy is lower in physics
126 gates). Therefore, reading a typical “cycle” (single physics gate plus single
127 calibration gate) requires 1.4 seconds. Calibration readout times are very
128 stable, but physics gate readout times vary with the level of activity in the
129 detector. The DAQ is programmed to protect the integrity of physics gates
130 above all else. It will only attempt a calibration readout in the case where
131 the physics readout is accomplished in under 0.9 seconds. If the subsequent
132 calibration readout extends beyond 0.9 seconds, the DAQ will dump that
133 readout and simply arm for the next physics spill. However, the DAQ will
134 not interrupt readout of a physics gate. Propagation of the start gate signal
135 is blocked in hardware and only unlatched after readout is complete.

136 3. System-Wide Timing Signals

137 Time-stamps are recorded for the MINER ν A experiment using a single
138 53.1 MHz crystal on the MvTM which is distributed to all of the electronics
139 components - from MvTM to the CRIMs, from the CRIM to the CROCs,
140 from the CROCs to the FEBs. See Fig. 1 for an illustration of the timing
141 signals loop. Each board regenerates the clock using phase-locked loop (PLL)

142 circuits. The 53.1 MHz clock is distributed on the readout cable, but the
 143 FEBs use the onboard PLL to multiply the frequency by two. All times in
 144 MINER ν A are defined in units of system ticks, or clock ticks. A clock tick
 145 is equal to

$$1/f = 1/(2 \times 53.1 \times 10^6 \text{ Hz}) = 9.4 \text{ ns} \quad (1)$$

146 Additionally the FPGA on the FEB uses a quadrature circuit, providing a
 147 granularity of ~ 2.4 ns for the discriminator time stamps. Throughout the
 148 remainder of this document, the term “clock tick” will refer to the unit used
 149 by the FEBs (~ 9.4 ns) unless explicitly noted otherwise.

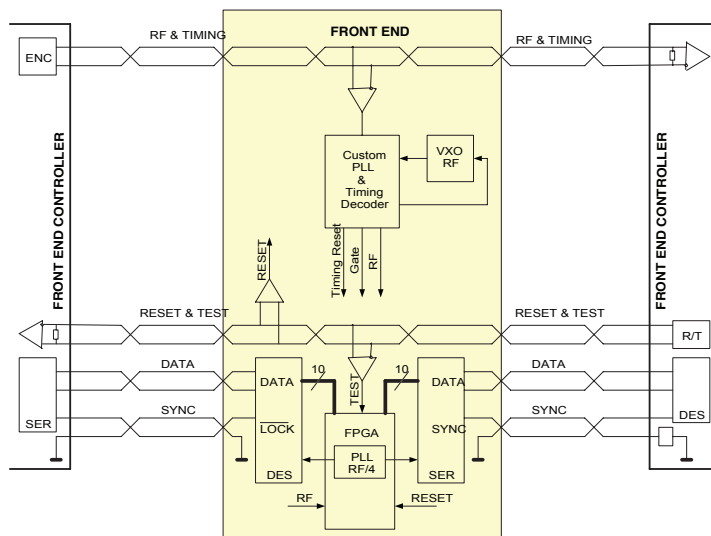


Figure 1: The DAQ Loop Timing Signals.¹³

150 The FEBs, CROCs and CRIMs can operate using on board oscillators,
 151 but FEBs and CROCs in MINER ν A are always operated by synchronizing
 152 their clocks to a radio frequency (RF) signal provided by the CRIMs. The
 153 CRIMs are typically operated in “MvTM Mode,” and locked to the MvTM
 154 clock, but in certain situations are placed in “Internal Mode,” where the
 155 clock is supplied by the internal crystal oscillator. See Table 3. MINER ν A
 156 electronics were designed to operate without a trigger, so the cosmic and
 157 Test-Beam modes are special. In those cases, a coincidence between a live
 158 gate ($\approx 16 \mu\text{s}$ wide) and an external logic pulse is searched for in order to
 159 make readout decisions. Because of dead-time between gates, the live-time
 160 is low in those operating modes ($\sim 10\%$).

Data-Taking Mode	CRIM Clock Mode
Pedestal	Internal
Cosmic Rays	Internal
FTBF (Test-Beam) Beam	Internal
NuMI Beam	MvTM
Light Injection (LI)	MvTM
Mixed Mode (Beam with LI or Pedestal)	MvTM

Table 3: CRIM timing modes for different data-taking modes. “FTBF” refers to the Fermilab Test Beam Facility.

161 When operating in the internal timing mode, each CRIM supplies its own
162 clock and either the DAQ system sends a new open-gate command after each
163 successful readout or the CRIM opens the gates independently at a frequency
164 set by the user ranging between 0.5 Hz and 52 kHz. The first sort of internal
165 clock mode operation is used for standalone pedestal runs and the second
166 requires an external trigger in coincidence to initiate readout (cosmic or test
167 beam).

168 Encoded clock and trigger signals enter the CROCs over LVDS via RJ-45
169 input connectors:

- 170 1. RF - Radio Frequency
- 171 2. SGATE - Start Gate (open an integration gate)
- 172 3. CNRST - Counter Reset
- 173 4. FCMND - Fast Command (special commands)
- 174 5. TCALB - Timing Calibration Pulse

175 See Fig. 2 for the structure of the encoded commands on the clock line.

176 In either Internal or MvTM timing mode, the CRIM can receive exter-
177 nal signals via a set of LEMO connectors on its front panel or via an RJ-45
178 connector. The MvTM is able to receive timing signals from the MINOS
179 Master Timing Module over UTP Cat5e using LVDS. The MvTM addition-
180 ally can send and relay Low Voltage Transistor-Transistor Logic (LVTTTL)
181 signals through the pairs of in-and-out LEMO connectors. One LEMO in-
182 put is used to receive a LVTTTL signal providing MI cycle status from the
183 Accelerator Division (this signal ultimately determines the start-gate time).
184 The other two LEMO connectors are used to fire the light injection system
185 (discussed later).

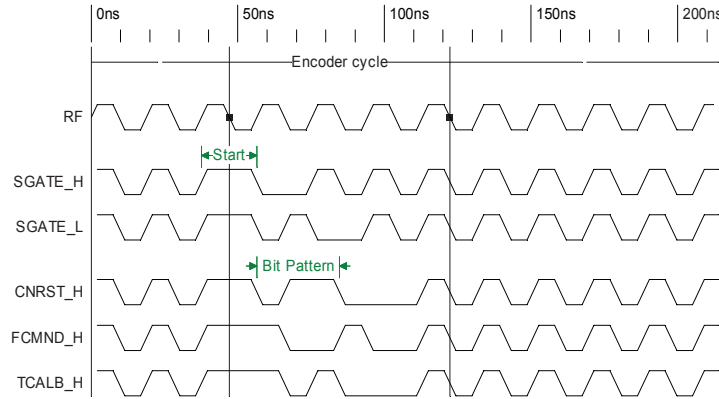


Figure 2: The Timing Encoder Signals.¹³

186 During normal operation, the CRIM clock is derived from the MvTM. In
 187 principle, the MvTM can sync to the MINOS clock signal but it runs free
 188 against that clock and the MvTM internal oscillator is used to synchronize
 189 all of the clocks. The arrival time of the MINOS start-gate signal is recorded
 190 in a register in the CRIM, however. The MINOS and MINER ν A clocks are
 191 therefore running in sync with an unknown phase shift. When in MvTM
 192 mode, the CRIM will raise an interrupt when an external trigger pulse is
 193 detected - for example, when the spill signal comes from the MI. This inter-
 194 rupt begins the readout sequence and blocks until it is reset after readout is
 195 complete. Fig. 3 illustrates the timing module logic.

196 The CRIM interprets Start-gate (SGATE), trigger (TRIG), timing cali-
 197 bration (TCALB), and counter-reset (CNRST) LVTTTL signals and generates
 198 corresponding output in a slightly different way for each of the different tim-
 199 ing modes.

- 200 1. SGATE is sent through SGATE OUT in all timing modes.
- 201 2. TRIG is sent only in MvTM mode, and only in case of a software
 202 command to open a gate.
- 203 3. TCALB is sent synchronously with SGATE in most CRIM firmware
 204 versions. It can be configured to only send this signal when an external
 205 TRIG is supplied.
- 206 4. CNRST is sent synchronously with SGATE in most CRIM firmware
 207 versions. The FEBs interpret this as a “Counter Load” signal and set
 208 their counters to a value specified in the FPGA programming registers.
 209 This is part of the timing synchronization scheme for the FEBs.

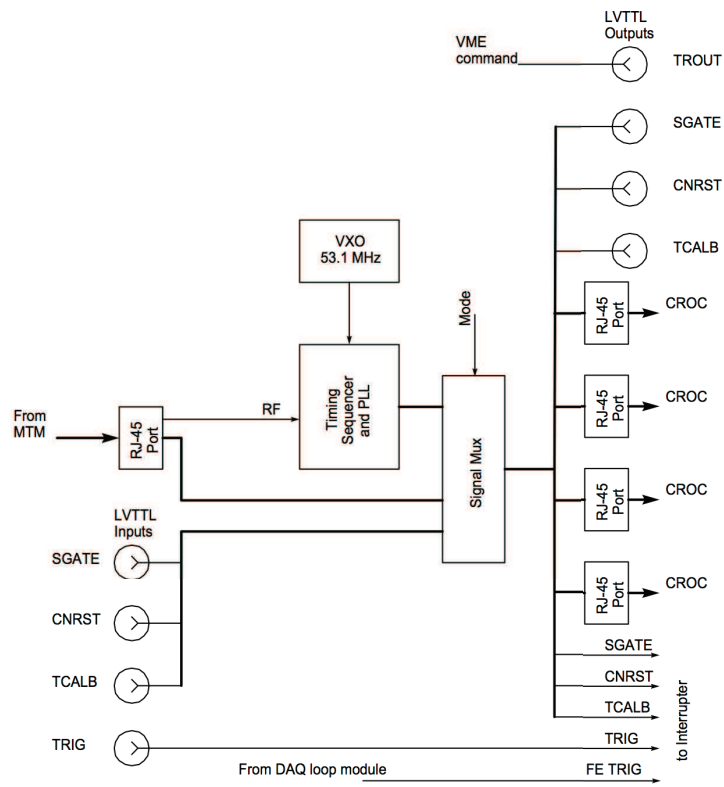


Figure 3: The CRIM (timing module) block diagram.¹⁴

210 The clock and data travel only in one direction over the readout chains- from
211 the CROC to each of the FEBs in turn and arriving back at the CROC. The
212 CROC checks that the clock is present at the receiving end and will set an
213 error flag if it is not. Further data acquisition is not possible until this error
214 is cleared.

215 Our configuration for data-taking in the NuMI hall is:

- 216 1. A LEMO cable from the accelerator division rack is attached to LEMO
217 input 1 on the MvTM. A signal synchronized with the MI operational
218 cycle arrives $\sim 215 \mu\text{s}$ before a spill. A delay is programmed into the
219 FEB FPGA's to account for the offset. This signal is sent to the CRIM
220 from the MvTM via a CAT3 cable, and propagated from there through
221 the CROCs to the FEBs. The FEBs use only the rising edge of the
222 SGATE signal to open a gate. The falling edge is ignored.
- 223 2. A dedicated CAT3 cable is routed from the MINOS clock rack into
224 the Master Clock Interface connector on the MvTM. This cable car-
225 ries CNRST, TCALB, and SGATE encoded clock signals. The CRIM
226 receives those signals as:
 - 227 • MINER ν A CNRST - MINOS CNRST. Set by the MINOS GPS
228 clock to reset asynchronous to the other signals at a rate of 1 Hz.
229 This signal is currently masked from the FEBs, but used to reset
230 the counter on the CRIM.
 - 231 • MINER ν A TCALB - The MINOS SGATE signal is mapped here
232 in the MvTM. The clock time is recorded (using on-board coun-
233 ters) for the arrival of this signal and stored on a register in the
234 CRIM that is read at the end of the acquisition cycle.
 - 235 • MINER ν A SGATE - This receiver is masked within the MvTM
236 and the CRIM never sees a signal of this type.
- 237 3. All of the CRIMs are daisy-chained together via the TRIG port, going
238 out from the "Master CRIM" (the CRIM with the lowest address in
239 the VME crate with the lowest address) and then in and out of all sub-
240 sequent CRIMs (incrementing by CRIM address before crate address)
241 until the input on the last CRIM (the CRIM with the highest address
242 in the VME crate with the highest address) is reached. This chain is re-
243 sponsible for propagating the start signal in light injection data taking.
244 A software command is sent to the Master CRIM only and propagated
245 to the others via this electrical connection. Additionally a signal is sent

246 from the Master CRIM SGATE connector to the light injection box.
247 This output is passed through the MvTM itself for shaping and delay.
248 4. The CRIM is run in one of two timing modes (see Table 3). In the
249 Internal and MvTM modes a sequencer that sends SGATE, TRIG,
250 and CNRST to the FEBs is employed. If running in “cosmic” mode for
251 the MINER ν A Test Beam Experiment, TCALB is additionally sent if
252 an interrupt was raised.

253 4. Hit Timing

254 The MINER ν A FEBs mount six TriP-t chips. Four are dedicated to the
255 high and medium gain and two are dedicated to the low gain. Due to this
256 division, the TriP-t chips must be grouped together when storing hits in order
257 to avoid some potential ambiguities. This has important consequences for
258 hit timing.

259 4.1. TriP-t “Push” Behavior

260 Understanding hit storage is important for understanding hit timing. The
261 TriP-t has a 48-cell deep analog pipeline and integrated charge is pushed into
262 this pipeline when the discriminator fires according to a process described be-
263 low. Each cell of charge corresponds to a “hit.” This behavior is not internal
264 to the TriP-t chip, but is controlled but the FPGA firmware. The readout
265 depth (number of total allowed hits) is limited by the internal memory of
266 the FPGA and the way digitized data from the hits is stored in the FPGA.
267 There is flexibility in the maximum number of hits that may be stored, but
268 in standard configurations prior to 2012, MINER ν A stored up to eight hits.

269 Charge is integrated over a time window set by the user. The whole
270 window is referred to as a “gate.” Activity is separated in time inside this
271 gate by latching the system counter when the integrated charge goes over
272 a user-defined threshold and then storing the charge integrated up to that
273 time (this process is called “pushing the pipeline”). After storing the hit,
274 the integrators are reset and re-opened. At the end of the gate, the analog
275 information stored in the pipeline is digitized into RAM with one ADC block
276 (or “hit”) for each stored set of charges in the pipeline (for each “pipe”).
277 The different times associated with these processes are tunable by the user.
278 In MINER ν A, the standard gate length is 1702 clock ticks ($\approx 16 \mu\text{s}$). The
279 integration time after a discriminator fires is 16 clock ticks ($\approx 150 \text{ ns}$), and
280 the reset requires 20 clock ticks ($\approx 188 \text{ ns}$).

281 The six TriP-t chips on each FEB are numbered 0-5, and each carries 32
282 channels. TriP-t chips 0-3 each operate 16 channels in the high gain mode
283 and 16 channels in the medium gain mode. TriP-t chips 4 & 5 each operate
284 32 channels in the low gain mode. There are 64 channels on each multi-
285 anode PMT, so TriP-t chips 0, 1, and 4 serve one half of the PMT, and
286 TriP-t chips 2, 3, and 5 serve the other. Note this means any given pixel on
287 a PMT is serviced by two separate TriP-t chips - one chip with one channel
288 operating in a low-gain mode (low amplification of signal), and one chip
289 with two channels, one in a medium-gain mode and one in a high-gain mode
290 (large amplification of signal). All three channels operate simultaneously and
291 independently of each other, each recording a value proportional to the gain
292 times the charge. In principle, every channel on a TriP-t chip supports a
293 discriminator, but only the discriminators on the high gain TriP-t channels
294 are active. This is because the high gain channels are the most sensitive
295 and low and medium-gain channels cannot be over threshold without their
296 corresponding high-gain channel also being over threshold. The channel map
297 ties two high and medium-gain TriP-t chips to each low gain TriP-t chip. In
298 order to associate data in the low gain with data in the high or medium
299 for a given channel, the low-gain TriP-t for that channel must be pushed
300 with the high gain TriP-t chip. To avoid ambiguous hit assignment for the
301 *other* channels serviced by the low-gain TriP-t chip that are not shared with
302 the firing high-gain chip, the “parallel” high-gain chip must also be pushed.
303 Thus, there are effectively two logical units, 32 channels in size, on each
304 board that are used to fill the analog pipelines.

305 *4.2. Clock Ticks and Time*

306 Time on the FEBs is set relative to a free-running counter that counts
307 up in clock ticks until it reaches the 32-bit unsigned integer maximum, at
308 which point it simply rolls over to zero. The counters are reset to the value
309 stored in the programming registers of the FPGA control chips when the
310 FEBs receive a CNRST signal. By tuning this start value to account for
311 signal propagation time, it is possible to synchronize the local counter values
312 on the FEBs to within one clock tick.

313 After a gate-open signal, the FEB loads its Timer register value and starts
314 a counter that counts up to the 16-bit unsigned integer maximum. This delay
315 is used to synchronize with beam activity and as a “quiet” period to blank
316 charge pulses to the CW voltage system just before SGATE (at least 15
317 microseconds is required). At the counter maximum the FEB gate opens

318 and the time on the free-running counter is latched as our gate start time.
319 It is an offline software convention to subtract this time from all subsequent
320 calculations on a board.

321 Because the low gain channels are shared across two high and medium
322 gain sets of channels, when the discriminators fire charge is pushed and stored
323 in groups of 32 channels. This means a hit in a given channel creates a
324 timestamp T_0 for the whole TriP-t chip via the high gain. That timestamp
325 is further shared across the “TriP-t Chip Group” (0, 1, and 4 share the same
326 base time, and 2, 3, and 5 share a separate base time). Subsequent hits
327 within the 16-tick integration window have differing delay and quarter ticks.
328 Crossing a discriminator threshold causes all three associated TriP-t chips to
329 push 16 FEB clock ticks later, regardless of subsequent hits.

330 When a discriminator fires, it sets its whole TriP-t chip group (0+1+4
331 or 2+3+5) to push 20 system ticks later. The entire group shares the base
332 integer time stamp for the earliest channel to fire on the group, and the
333 initiating channel also stores a quarter-tick for fine resolution. The system
334 clock continues to run and provides delay and quarter ticks to timestamp
335 subsequent hits (prior to the push) to 1/4 of a tick accuracy in other channels
336 (pixels) in the group.

337 4.3. Dead Time

338 Coupling pairs of high gain TriP-t chips implies dead time impacts 32
339 channels at a time. The reset after a push requires 20 clock ticks to complete.
340 During the reset period, all three TriP-t chips that pushed are essentially dead
341 to incoming signals. Hits during the reset period are un-timed and the charge
342 recorded is either greatly attenuated or zero. For illustration, consider Fig.
343 4. When there is a hit on one half of a discriminator-active TriP-t pair at
344 time T_0 and another hit at a later time T_1 , the second hit is latched in time
345 as long as it arrives before the push. If the second hit on either pair of TriP-
346 t chips arrives more than 16 ticks after the initiating hit, the later hit is not
347 recorded. Time on both TriP-t chips is relative to T_0 , the first threshold cross
348 between the two. Fig. 5 shows a typical bank structure for a gate and Fig.
349 6 shows the memory structure of a discriminator bank.

350 There is another form of dead time due to hit saturation. This occurs
351 when the number of “pushes” allowed by the pipeline depth are exhausted.
352 In this case, charge continues to integrate, but additional hits are no longer
353 time-stamped.

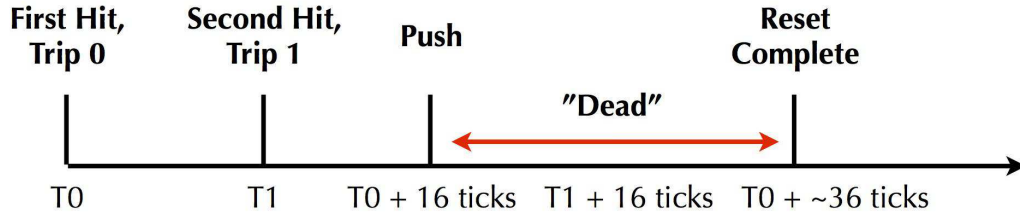


Figure 4: A specific dead-time illustration on one FEB. Consider a hit on TriP-t0. This hit will set a timestamp, T_0 here, and cause a pipeline push 16 clock ticks later for TriP-t chips 0, 1, and 4. A later hit at time T_1 above does not initiate a new pipeline push and the time is stamped relative to T_0 . The ADCs are effectively dead between $T_0 + 16$ and $T_0 + 36$ clock ticks. After that point, the ADCs on those TRiPs are fully live again and new hits over threshold will be timestamped.

Discriminator Bank (Header Info with # of Hits per TriP-t)		ADC Bank ("Hit X")	ADC Bank ("Hit X+1")
All hits for TriP-t 0	Hit 0	TriP-t 0	TriP-t 0
	Hit 1	PipeDelay - Hit 0	PipeDelay - Hit 1
All hits for TriP-t 1	Hit 0	TriP-t 1	TriP-t 1
	Hit 1	PipeDelay - Hit 0	PipeDelay - Hit 1
All hits for TriP-t 2	Hit 1	Garbage (read anyway)	TriP-t 2 PipeDelay - Hit 1
All hits for TriP-t 3	Hit 1	Garbage (read anyway)	TriP-t 3 PipeDelay - Hit 1

Figure 5: A generic example of the organization of data within the discriminator and ADC banks. The columns ("Hit X") denote hit RAM Functions - all of the data in the column is read at once and partial pipeline reads cannot be performed. In this case, there was a hit on either TriP-t0 or 1, another independent hit on either TriP-t2 or 3, and a final hit on TriP-t0 or 1. The ADCs cannot distinguish which TriP-t in the two pairs contained the initial hit for that pair. Again, this diagram does not distinguish which TriP-t had the channel hit first, and it cannot distinguish which of the hits in the "Hit 1" RAM Function was earlier - the discriminator bank must be decoded for that information. The end of integration "hit" is not included in the set of ADC banks shown here. It would appear in a new column titled "Hit 2" and would appear in all TriP-t's. For each FEB read out, the following RAM Functions: ReadDiscr, ReadHit0, ..., ReadHit7 are looped through.

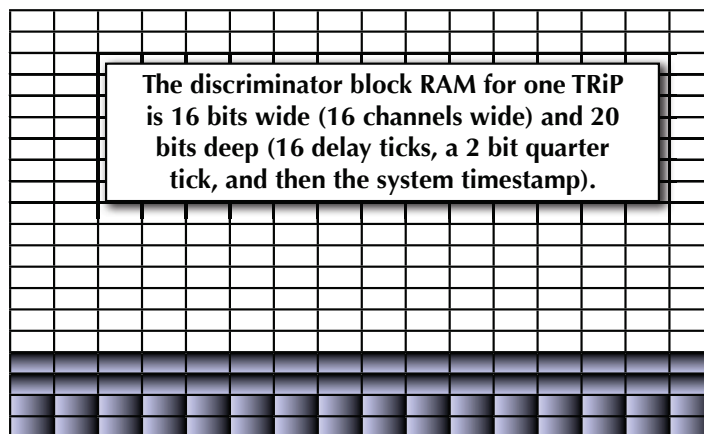


Figure 6: A visualization of the discriminator bank for a single TriP-t chip. The system tick is stored in the 32 bits at the “bottom” of the figure. Quarter ticks for each channel are stored in the 32 bits above that at 2 bits per channel. Finally, the delay ticks are stored in 16 bits for each channel above the quarter ticks.

354 4.4. FEB Timing Synchronization

355 When the CRIM sends an open-gate command (SGATE) through the
 356 CROCs to the FEBs, the actual signal arrives at different times to the dif-
 357 ferent FEBs on the chain due to cable delays. This is accounted for in two
 358 steps:

- 359 1. The FEB loads the value recorded in the Timer register of the FPGA.
 360 By staggering the time loaded to account for the finite signal propaga-
 361 tion time down the chain, all of the boards can synchronize the values
 362 on their local counters.
- 363 2. Once the FEBs receive an open-gate signal they begin counting up
 364 to a pre-set open-gate time value, beginning not with zero, but with
 365 the Timer value mentioned in the previous step. This additional delay
 366 is meant to provide the PMT with time to settle into a stable high
 367 voltage in the case the Cockroft-Walton adjusted the voltage period
 368 just before the gate is opened. Once they reach this time, they open
 369 their integration gates. All the FEBs will physically open their gates
 370 at the same local time.

371 5. DAQ Software

372 5.1. Readout Control

373 The DAQ is a system built out of three computers running 64-bit Scientific
374 Linux Fermi¹⁵ - one readout node for each VME crate and one master node.
375 Data transfer between the readout nodes and master node is handled via the
376 Event Transfer (ET) software package (part of CODA¹⁶), discussed further
377 below. The head node initiates a run and creates a memory-mapped file to
378 store data. It provides instructions to the readout nodes on when to begin
379 the readout sequence. When readout begins, each of the slave nodes passes
380 data frame-by-frame to the master for collation. At the end of a run, the head
381 node converts the memory-mapped file into a flat binary and releases it. One
382 feature of this approach is that if the DAQ fails during readout, the collected
383 data are already stored on disk and are not lost. The DAQ is written in C++
384 to run on Scientific Linux Fermi¹⁵, but should run with minimal modifications
385 on most major Linux distributions. The code is divided into four libraries:

- 386 1. Hardware access: Our hardware access libraries are built on top of a
387 set of proprietary (closed-source) libraries provided by CAEN to access
388 the V2718 VME crate controller⁹ using the A2818 PCI optical bridge
389 card¹¹. Functions from the libraries CAEN makes freely available for
390 this hardware on its website are used to format command and control
391 messages to the CROCs and CRIMs as required during readout.
- 392 2. Event structure: Another set of libraries that define the types and
393 structures of the MINER ν A data types.
- 394 3. Acquisition control: These libraries and executables run the acquisition
395 and interface with the Run Control software described in Section 5.2.
- 396 4. Buffer management and interprocess communication (IPC): Like the
397 hardware access libraries, the buffer management and IPC code uses
398 external libraries. In particular, the open-source Event Transfer (ET)
399 system version 9.0, based on CODA,¹⁶ developed at the Thomas Jef-
400 ferson Lab National Accelerator Facility (JLab)¹⁷ is used.

401 5.2. Run Control

402 The run control is written in Python for flexibility and platform-independence.
403 There are two external Python libraries (in addition to the DAQ software,
404 described in section 5.1) needed for various components of the run control to
405 work:

- 406 1. wxPython¹⁸, chosen as our graphics toolkit because of its ease of use
407 and maturity;
- 408 2. pySerial¹⁹, which provides a convenient RS-232 interface.

409 **6. Computing Architecture**

410 *6.1. Overview of Data Handling*

411 MINER ν A uses two networks of server-class computers: one for physics
412 data collection and one for data quality monitoring and run control. The
413 data collection PCs are detailed in Section 7. For monitoring, MINER ν A
414 uses two remote clusters of computers at Fermilab: one in the Feynman
415 Computing Center (FCC), and the other at Wilson Hall (WH). These systems
416 are discussed in Sections 8 and 9

417 Data are collected and logged underground independently of above-ground
418 computing clusters. The DAQ can run without input from or a connection
419 to any above-ground network with local storage for physics data, metadata,
420 and logs sufficient for about a month of normal operations. The above-
421 ground computers manage long-term data archival, log file metadata into
422 SAM (Sequential Access Method - a metadata database application)²⁰, pro-
423 duce histograms for monitoring, and provide run control options.

424 *6.2. Data acquisition coordination*

425 The run control software manages connections between most of the com-
426 puters used in the data acquisition and monitoring process such that they
427 remain synchronized throughout. Kerberos-authenticated²¹ SSH tunnels are
428 used to connect clients (i.e., user shift consoles) to a master DAQ server pro-
429 cess and the master DAQ server to the other slave machines, as described
430 below.

431 The heart of the run control is a central server process on the master
432 DAQ node. It maintains communication with “dispatcher” processes running
433 on each of the relevant slave remote nodes so as to instruct them to start
434 or stop their various tasks as the state of data acquisition changes. It is
435 also the entry point for communication from the graphical end client used
436 by operators to interact with the DAQ. This “DAQ manager” process can
437 coordinate data taking irrespective of the number of clients connected; once
438 started, it will run through to completion of the data acquisition sequence
439 even if the controlling client is disconnected.

440 The DAQ manager connects to a collection of remote nodes in various
441 locations. Among these are readout nodes that insert the digitized data
442 into the data stream and the monitoring nodes that run slow monitoring
443 processing jobs and serve the data to the operator.

444 Operators control the DAQ using a graphical client (also contained in the
445 run control package) that connects to the DAQ manager over the network
446 using a custom thin-client TCP protocol. This design accommodates both
447 the Fermilab control room and collaborator institutions located around the
448 world.

449 **7. Physical Organization of the Readout Equipment in NuMI**

450 All relevant MINER ν A electronics equipment is mounted in racks sitting
451 on a deck beside the detector. All racks are equipped with smoke detection
452 and interlocked power, with rack protection and slow monitoring built into
453 the overall online scheme.

454 Racks are labeled according to their primary hardware electronics com-
455 ponents and there are four primary racks:

- 456 1. The VME Rack (also sometimes called the DAQ Rack)
- 457 2. The Light Injection (LI) Rack
- 458 3. The Veto Rack
- 459 4. The Spares Rack

460 Our racks all consume less than 2500W each, meeting the FNAL require-
461 ments for air cooling. See Fig. 7 for an overview of the arrangement of and
462 connections between the three racks.

463 *7.1. The VME Rack*

464 The VME Rack contains the two VME crates that hold the MINER ν A
465 readout electronics. It additionally mounts a pair of PCs and network sup-
466 port components. Access control for devices that cannot be configured to use
467 Kerberos is provided by a very restrictive ACL (Access Control List). See
468 Fig. 8 for the rack layout and connection types. Insofar as the readout ar-
469 chitecture is concerned, it contains (roughly in mechanical installation order
470 from top to bottom):

- 471 1. A custom Temperature and Environment Monitor (TEM) device (la-
472 beled the “Slow Monitor”) that supports eight temperature probes that

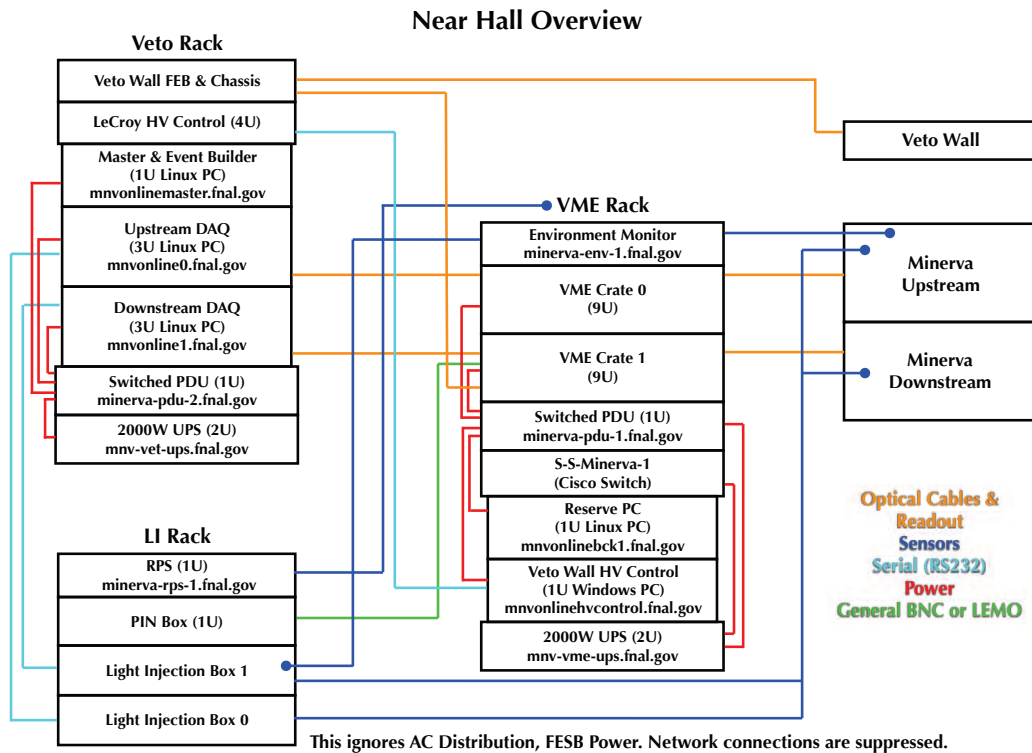


Figure 7: Connection map for the MINERνA readout system, ignoring AC distribution, FESB power, and safety systems. Network connections are also suppressed - every device with an internet name is linked to the network switch housed in the VME rack.

- 473 may be deployed throughout the racks and over the detector surface.
474 The device also logs humidity, pressure, and temperature at the end of
475 six cabled sensors deployed on the detector.
- 476 2. Two CAEN VME 8011 crates²². The crates are indexed as 0 and 1.
477 Crate 0 contains a controller module, two CRIM modules, and eight
478 CROC modules. Crate 1 contains a controller module, two CRIM
479 modules, seven CROC modules, and a MvTM module. See Figs. 9
480 and 10 for the VME module assignment in Crates 0 and 1 respectively.
 - 481 3. An APC 120VAC Masterswitch III Switched Rack PDU (Power Distri-
482 bution Unit), Model # AP7900. This PDU is a networked device that
483 provides remote power control for the VME crates and all PCs in the
484 rack.
 - 485 4. A 48 port Cisco C2960G switch, designated S-S-MINERVA-1.²³
 - 486 5. Three 48VDC power supplies to power the FEB's (not pictured in the
487 figures).
 - 488 6. Three networked fuse panels for the 48VDC power supplies, networked
489 to S-S-MINERVA-1. These fuse panels host a web interface with self-
490 documented power control of the FESBs mounted on the MINERVA
491 detector (not pictured in the figures).
 - 492 7. A 1U Linux PC serving as a back-up for the master DAQ node in the
493 Veto Rack (see Section 7.3).
 - 494 8. A 1U Windows PC running control and monitoring software for the
495 LeCroy High Voltage Power System (HVPS) located in the Veto Rack.
496 *Not currently installed. Space, power, and networking resources are*
497 *reserved.*
 - 498 9. An APC Smart-UPS 2200VA (2000W Un-interruptible Power Supply)
499 supporting the switch and PCs. The primary function of this UPS is
500 power filtering. In the event of a full power failure, the system will
501 remain live for more than thirty minutes.

502 7.2. The LI Rack

503 The LI rack contains the MINERVA custom-built Light Injection (LI)
504 boxes²⁴. The rack is intentionally kept sparse to provide sufficient space to
505 route and store the optical fibers that connect from the back of the LI boxes
506 to the PMTs mounted on top of MINERVA. See Fig. 11 for the rack layout
507 and connection types. For our purposes, it contains (roughly in mechanical
508 installation order from top to bottom):

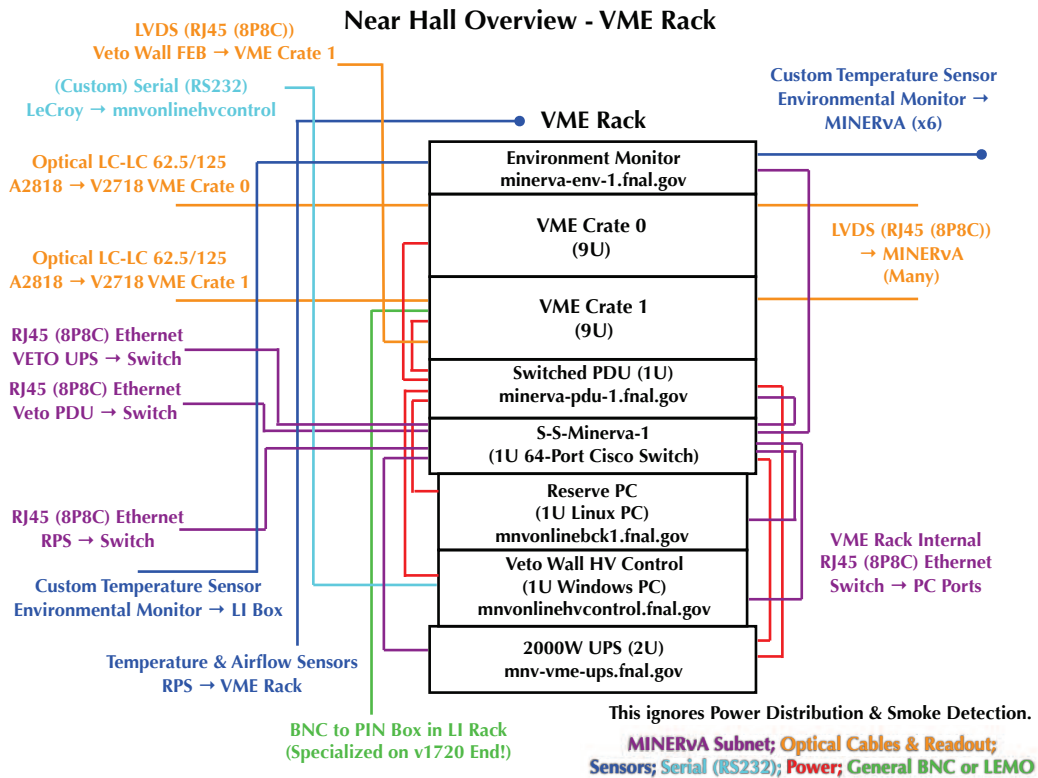


Figure 8: Connection map for the VME Rack. Power architecture is not shown, including the three networked fuse panels.

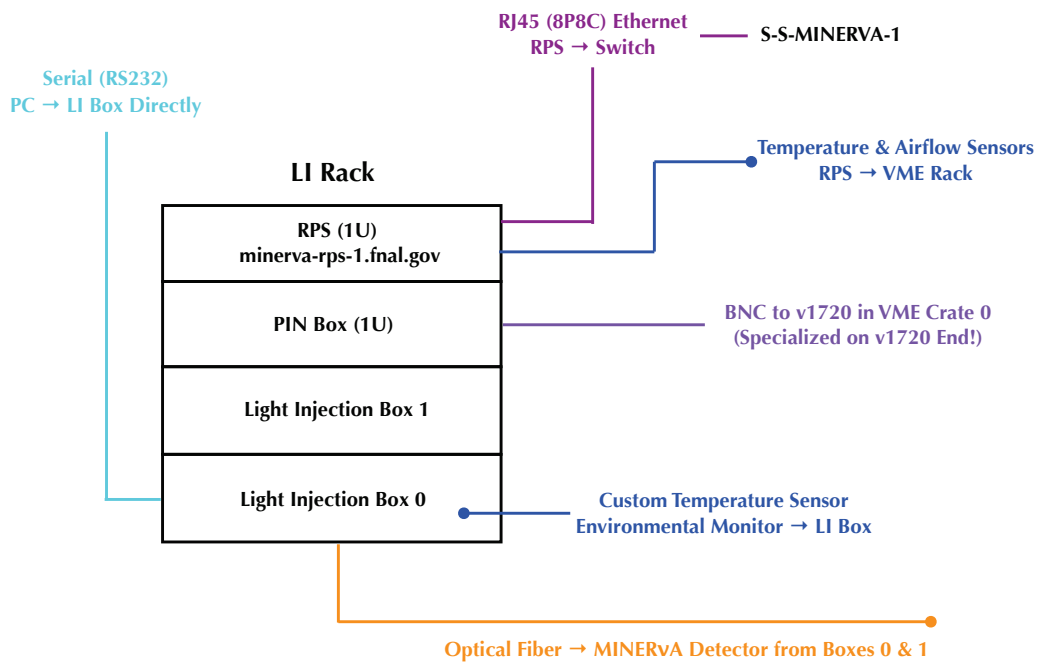
- 509 1. A BiRa Rack Protection System (RPS). The RPS deploys a variety
510 of monitoring cables into the VME Rack: voltage-monitoring cables
511 to the VME crates, and airflow and temperature sensors. The RPS is
512 connected to the S-S-MINERVA-1 switch located in the VME rack by
513 ethernet.
- 514 2. A PIN diode box. The PIN is optically connected to the LI box to
515 monitor the stability of the LED light output. The PIN box is addi-
516 tionally connected via BNC and specialized cables to a CAEN V1720
517 waveform digitizer²⁵ mounted in VME Crate 0 in the VME Rack.
- 518 3. The primary LI box. This box contains control electronics and LEDs
519 that service optical connectors on the back of the box. From those
520 connectors light is piped via optical fiber to the PMT boxes mounted
521 on top of the detector. It is interfaced via a 9-pin serial RS-232 socket
522 on the front of the box. This serial cable is connected to the MINER ν A
523 DAQ PC cluster for configuration commands. It additionally accepts
524 a LEMO connection for the external trigger signal.
- 525 4. A secondary (smaller) LI box to service the most forward detector
526 modules. It uses the same electronics and connections as the larger
527 box, but mounts fewer LEDs.

528 *7.3. The Veto Rack*

529 The Veto rack derives its name from the LeCroy High Voltage Power
530 System mounted there that controls the high voltage on the resistor-base
531 PMTs deployed to readout the "Veto Wall" sitting in front of the MINER ν A
532 detector. It also contains the main readout PCs for the DAQ system. See
533 Fig. 12 for the rack layout and connection types. For our purposes, its
534 important contents are:

- 535 1. Two MINER ν A FEBs attached to a special custom breakout board
536 in a 2U chassis. The FEBs are standard MINER ν A boards, but the
537 breakout board is required to interface the single-anode PMTs (resistive
538 base) used to monitor the scintillator panels in the veto wall.
- 539 2. A LeCroy Model HV4032A High Voltage Power System (HVPS). The
540 HVPS connects to the readout PC located in the VME Rack via a
541 special custom serial cable. It also connects to the Veto Wall PMTs.
- 542 3. A 1U Linux PC running the DAQ Master software. This PC is identical
543 to the logger PC in the VME Rack. The DAQ Master node connects
544 to the Slave Readout nodes via direct ethernet.

Near Hall Overview - The Light Injection (LI) Rack



This ignores Power Distribution & Smoke Detection.

MINERVA Subnet; Optical Cables & Readout; Sensors; Serial (RS232); Power; General BNC or LEMO

Figure 11: Connection map for the LI Rack.

- 545 4. Two 3U Linux PCs serving as DAQ Readout Slave nodes. Each PC
 546 mounts a CAEN a2818 PCI Optical Bridge card¹¹ and interfaces with
 547 one of the VME crates located in the VME Rack.
- 548 5. An APC 120VAC Masterswitch III Switched Rack PDU (Power Distri-
 549 bution Unit), Model # AP7900. This PDU is a networked device that
 550 provides remote power control for the VME crates and all PCs in the
 551 rack.
- 552 6. An APC Smart-UPS 2200VA (2000W Un-interruptible Power Supply)
 553 supporting the PCs. The primary function of this UPS is power filter-
 554 ing. In the event of a full power failure, the system will remain live for
 555 over thirty minutes.

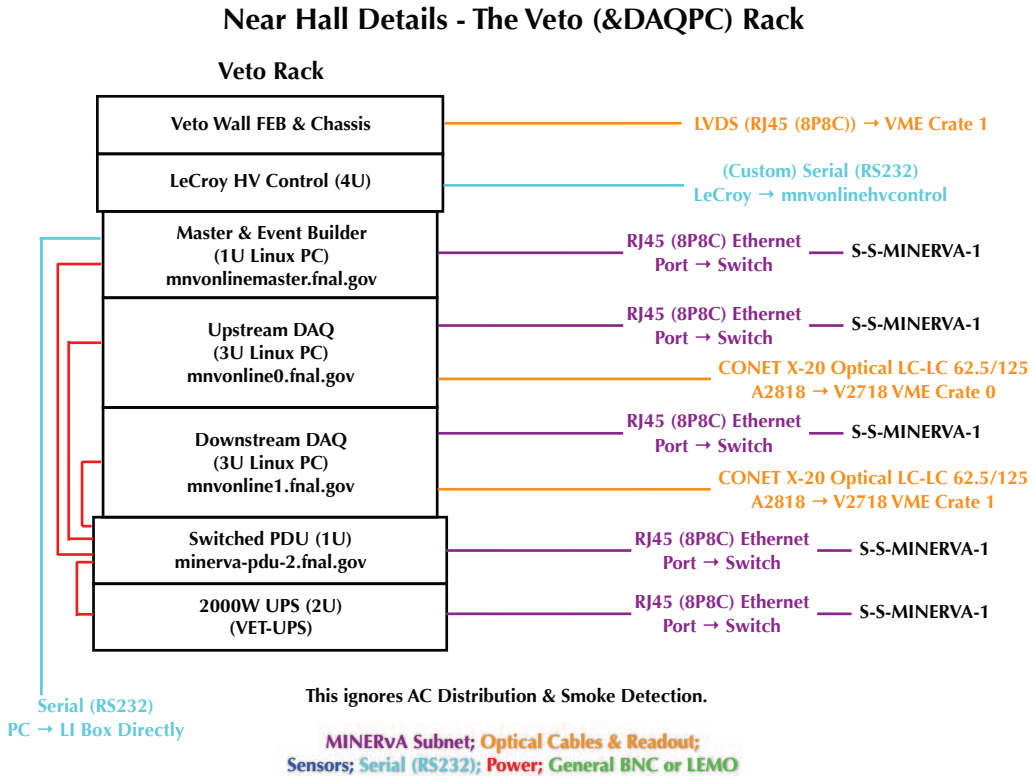


Figure 12: Connection map for the Veto Rack.

556 *7.4. The Spares Rack*

557 The final rack in the MINER ν A electronics installation sits across the hall
558 from the detector on the West side of the enclosure. It contains a number of
559 spare components:

- 560 1. A 3U Linux PC configured to serve as a spare readout node.
- 561 2. A 48 port Cisco C2960G switch, designated S-S-MINERVA-2.²³
- 562 3. A 1U Linux PC running logging software for the slow monitoring de-
563 vices. This machine also serves as the head node for a pool of servers
564 running a Condor²⁶ queue for batch processing jobs used to support
565 monitoring activities in the control room.
- 566 4. Spare AC distribution and smoke protection units.

567 *7.5. Power Infrastructure*

568 *7.5.1. DC Power Distribution*

569 The large number of Front End boards and their location atop the de-
570 tector makes conventional low-voltage power distribution impractical. A dis-
571 tributed power architecture is employed where 48 VDC power equipment
572 is located in the electronics racks and intermediate low voltage regulation is
573 performed on the detector near the FEBs. Finally, low-noise linear regulators
574 on each FEB produce the final 3.3 V power required.

575 Each FEB readout chain (up to ten FEBs) is powered by a Front End
576 Support Board (FESB) which contains an isolated DC-DC converter to step
577 down 48 VDC to approximately 4 VDC at 20 A. FESBs are passively cooled
578 and use the FEB/PMT steel mounting bracket as a heat sink.

579 Three 48 VDC power supplies operate in parallel and support “hot swap”
580 and dynamic load sharing. Two supplies are required to meet the design
581 specification of 3000W. The extra power supply allows for “N+1” redundant
582 operation, which makes it simple to remove and replace a supply without
583 interruption. Each power supply is rated for 1900 W and provides an interface
584 by which the health of the supply may be monitored remotely (through the
585 Rack Protection System (RPS) interface board and Environmental Monitor).

586 Through the Fuse Chassis the main 48 VDC 120 A bus is fanned out into
587 six 20 A connections. Two of these 20 A connections feed a Network Fuse
588 Panel (NFP), which fans out into twenty 2 A busses going to the FESBs.
589 Each NFP offers independent control and monitoring of the FESBs through
590 a web interface.

591 The actual power supply consumption is 1500 W when the FEBs are
 592 idle. The redundant “N+1” power supply configuration has been robust and
 593 reliable and has operated continuously without problems since commissioning
 594 in 2008. See Fig. 13 for a schematic.

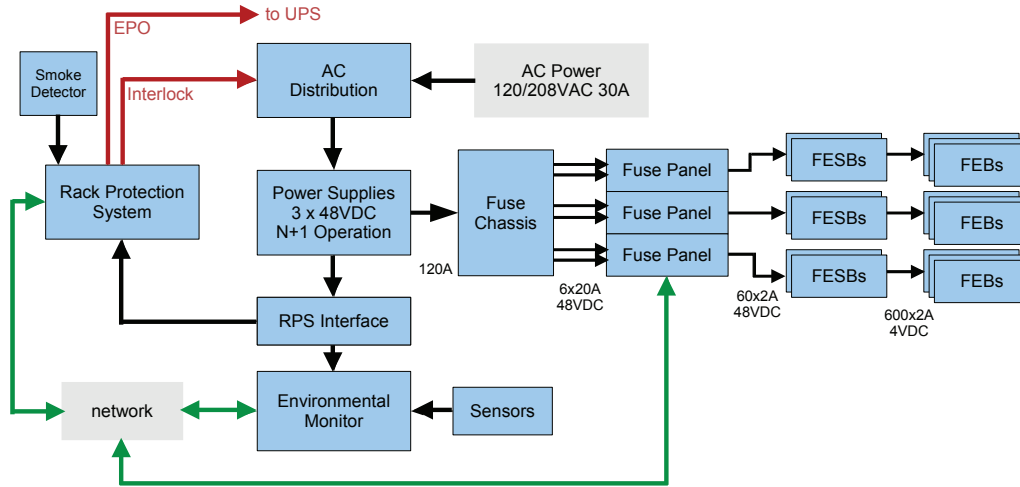


Figure 13: Power distribution for MINERνA.

595 7.5.2. Rack Protection System and AC Power Distribution

596 Rack protection is provided by the BiRa Systems RPS unit model 8884²⁷,
 597 which monitors a smoke detector in each of the three racks on the platform.
 598 If smoke is detected, the RPS unit drops the interlock signal, disabling the
 599 AC distribution chassis. The RPS also generates an emergency power output
 600 (EPO) signal that immediately disconnects the internal batteries on the UPS.

601 The Environmental Monitor reads various temperature sensors located
 602 around the detector. In addition, this monitor records and logs humidity and
 603 ambient light conditions. It is accessed through a web and FTP interface on
 604 the DAQ network.

605 8. Interface to the MINERνA Control Room

606 8.1. The MINERνA Control Room

607 The MINERνA control room is located in Wilson Hall at FNAL, in the
 608 north-west corner room on the 12th floor (WH12). See Fig. 14 for a map
 609 of building locations at Fermilab. MINERνA services our control room with

610 a total of eight PCs, with four in the Control Room and four in the Feyn-
 611 man Computing Center (FCC) at FNAL. The PCs kept in FCC run more
 612 processor-intensive tasks using a private Condor batch queue system²⁶.

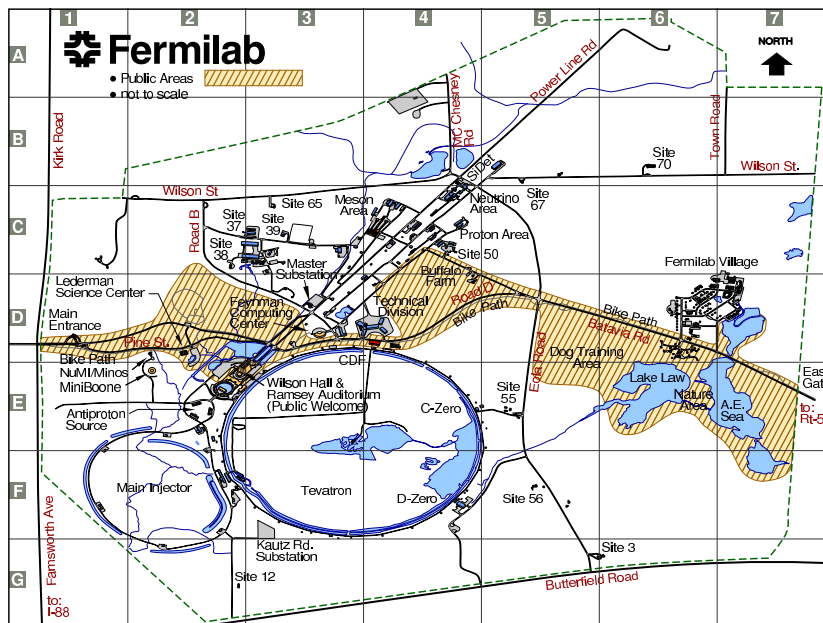


Figure 14: Buildings and sites at Fermilab.

613 8.2. Controlling the DAQ System

614 As noted above in section 6.2, the DAQ system is controlled via a graphi-
 615 cal thin client delivered with the run control software. The client runs locally
 616 on the operator’s terminal. Control of the DAQ is via a custom TCP thin-
 617 client protocol that is transmitted over a Kerberos-enabled SSH tunnel to
 618 the master DAQ node. Inbound connections are filtered both via the firewall
 619 provided by the NuMI router and by an access list of Kerberos principals
 620 allowed to log into the machine.

621 Commands sent via a successful tunnel to the DAQ manager process
 622 (running on the DAQ master node) are interpreted based on a notion of client
 623 “control” of the DAQ. At most one (though possibly zero) client(s) can be in
 624 control of the DAQ at any given time; only commands that originate from a
 625 node which is currently “in control” are ultimately acted upon. An unlimited

626 ³ number of clients are allowed to connect as observers. Any observer is
627 allowed to request control at any time; however, if another client is in control
628 at the time the request is made, the client in control is given a configurable
629 length of time to veto the request or approve transfer of control. In addition,
630 the run control package contains a client manager program that can revoke or
631 assign control to or from any client that is currently connected after proper
632 credentials are submitted, currently a password.

633 Once connected and in control, the operator is presented with a graphi-
634 cal interface containing details about the current data acquisition sequence
635 and status as well as controls allowing him/her to start, manually advance,
636 or stop data acquisition. When the DAQ is stopped the operator can also
637 adjust a handful of simple configuration options pertaining to the data ac-
638 quisition sequence he/she would like to begin. The bulk of the configuration
639 operations, however, is accessible only to experts directly on the DAQ head
640 node so as to avoid accidental misconfiguration.

641 Once initiated, data acquisition requires no intervention from the oper-
642 ator. The run control system can even operate unsupervised by any clients
643 at all (as would happen, for example, in the case where the network connec-
644 tion to a remote site is interrupted). Under these circumstances warnings
645 about the system state are queued and delivered in bulk to every client who
646 reconnects until they are acknowledged.

647 **9. Data Handling Paths**

648 The MINER ν A electronics are capable of monitoring a wide variety of
649 configuration states: high voltage on the (Cockcroft-Walton) PMTs deployed
650 on the detector, whether individual boards are dead or live, and the temper-
651 ature of the FEBs. A separate system monitors the resistive base PMTs used
652 for the MINER ν A Veto Wall. For cost-saving reasons MINER ν A uses the
653 same communications chain for electronics configuration and slow controls
654 as it does for data handling. As a consequence, these monitoring data are
655 packaged with the physics data directly and exist as part of that stream.

656 For monitoring purposes, the MINER ν A near-online, or “Nearline,” clus-
657 ter runs an ET client that is notified about the beginning and end of runs.

³Unlimited at least in principle. Network bandwidth and CPU time saturation, of course, will create an operational ceiling, though the actual maximum will depend on the environmental conditions.

658 During a run, it reads data from the DAQ head node frame-by-frame. When
 659 it completes an event (signified by reading the DAQ event header frame)
 660 it converts the binary data into MINER ν A “RawDigits” (the most basic
 661 analysis data format) for monitoring. Other tasks running on the Nearline
 662 cluster decode the RawDigits and process them through the MINER ν A soft-
 663 ware framework - producing monitoring quantities ranging from high voltage
 664 status to event displays. These are published to control room PCs for exper-
 665 imenters to study.

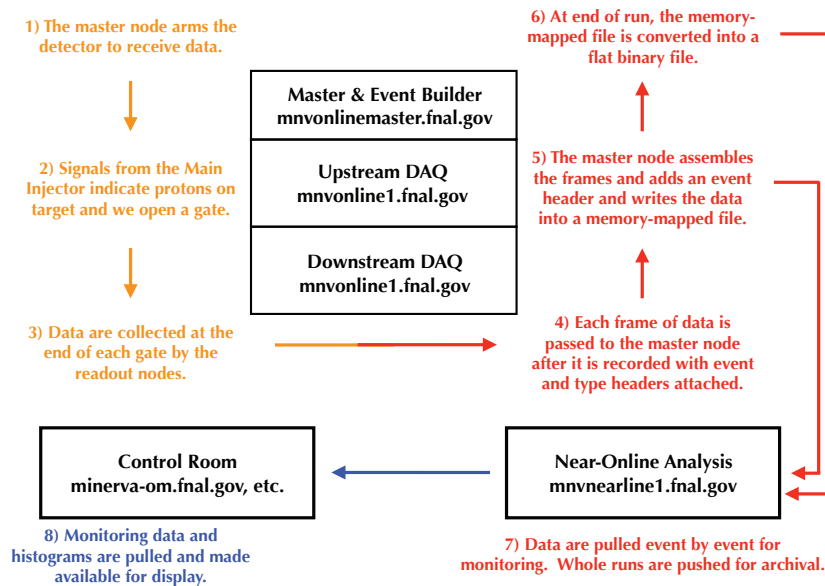


Figure 15: Flow-chart diagram for physics data through the MINER ν A acquisition chain. Not shown are the archival data handling beyond the near-online cluster or the metadata handling.

666 After each run a copy of the raw binary data file is pushed to the disk
 667 and tape for permanent storage. See Fig. 15 for a flowchart of the scheme.
 668 A long-term rolling copy of recent raw data is kept on the DAQ system itself
 669 (extending back approximately two months). With the raw data the DAQ
 670 additionally pushes metadata about the run for entry into SAM. Finally, a
 671 “keep-up” processing that uses raw data copied directly from the DAQ (not
 672 from the Nearline system) is also run to produce the RawDigits of record. In
 673 the end, there are three copies of the “raw” data at the end of this process:
 674 a copy of the raw data on the DAQ storage disks, a copy of the raw data in

675 permanent storage, and a copy of the RawDigits (raw data reformatted for
676 MINER ν A software consumption) for general use.

677 10. Summary and Performance

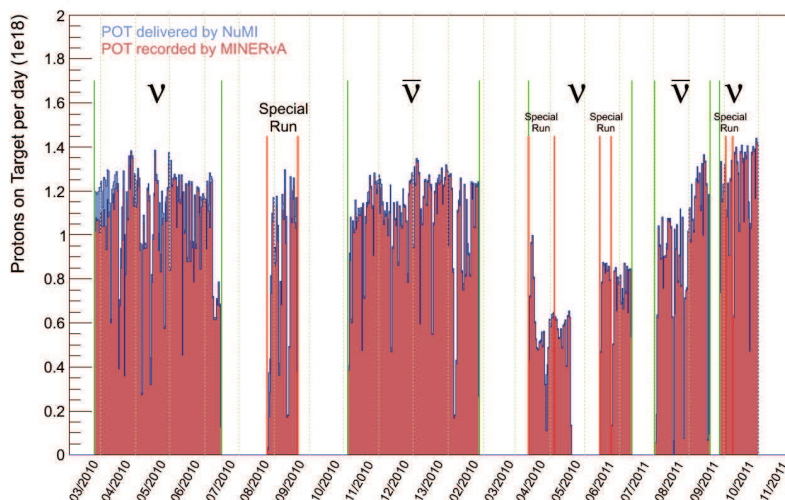


Figure 16: Protons on target delivered and recorded for MINER ν A.

678 MINER ν A began its official physics run on March 23, 2011 with the DAQ
679 system described above. Since that time, live-time for the whole period was
680 96.4% (not counting beam down-times). See Fig. 16 for a summary of the
681 protons on target delivered and recorded for MINER ν A. During normal op-
682 erations the live-time is over 99% and inefficiencies are almost entirely due
683 to change-over between runs. Our integrate live-time is most impacted by
684 electronics failures and simple operator error or inattention. There are ideas
685 for removing losses due to run change-overs (pre-starting the subsequent run
686 and putting it into a wait state to speed up the change) and our run control
687 system is constantly being improved to minimize the opportunity for exper-

688 imenters to make mistakes when running the system while still providing
689 flexible operational control.

690 **References**

- 691 1. The MINERvA Conceptual Design Report. MINERvA Doc-DB 482;
692 2006.
- 693 2. The MINOS Experiment. <http://www-numi.fnal.gov/Minos/>; 2011.
- 694 3. The NuMI Beamline. [http://www-](http://www-numi.fnal.gov/numwork/numiwk.html)
695 [numi.fnal.gov/numwork/numiwk.html](http://www-numi.fnal.gov/numwork/numiwk.html); 2011.
- 696 4. The MINERvA Technical Design Report. MINERvA Doc-DB 700; 2006.
- 697 5. Hamamatsu M64 PMT. [http://sales.hamamatsu.com/en/products/electron-](http://sales.hamamatsu.com/en/products/electron-tube-division/detectors/photomultiplier-tubes/part-r7600-00-m64.php)
698 [tube-division/detectors/photomultiplier-tubes/part-r7600-00-m64.php](http://sales.hamamatsu.com/en/products/electron-tube-division/detectors/photomultiplier-tubes/part-r7600-00-m64.php);
699 2011.
- 700 6. C.Gingu , P.Rubinov . Minerva Master/Slave Data Acquisition Board
701 Description and Measurement Result. 2005.
- 702 7. Rubinov P. AFEII Analog Front End Board Design Specifications. 2005.
- 703 8. Baldin B. VME Data Acquisition Modules for MINERvA Experiment.
704 FERMILAB-TM-2458-PPD; 2010.
- 705 9. The CAEN v2718 VME Crate Controller.
706 <http://www.caen.it/nuclear/product.php?mod=V2718>; 2008.
- 707 10. T.Fitzpatrick , C.Rotolo . MINOS Master Clock System Preliminary
708 Design Specification. NUMI-NOTR-ELEC-827, Fermilab; 2000.
- 709 11. The CAEN a2818 PCI Optical Bridge.
710 <http://www.caen.it/nuclear/product.php?mod=A2818>; 2008.
- 711 12. <http://www-d0.fnal.gov/>; 2011.
- 712 13. Baldin B. MINERvA Chain Readout Controller. MINERvA Doc-DB
713 1516; 2007.
- 714 14. Baldin B. MINERvA CROC Interface Module. MINERvA Doc-DB
715 1238; 2009.

- 716 15. Fermi Linux. <http://fermilinux.fnal.gov/>; 2011.
- 717 16. CODA. https://coda.jlab.org/wiki/index.php/Main_Page; 2011.
- 718 17. <http://www.jlab.org>; 2011.
- 719 18. <http://wxpython.org>; 2011.
- 720 19. <http://pyserial.sourceforge.net/>; 2011.
- 721 20. http://d0dbweb.fnal.gov/sam_pyapi; 2011.
- 722 21. <http://web.mit.edu/kerberos/>; 2011.
- 723 22. The CAEN 8011 VME Crate. [http://www.caen.it/nuclear/syproduct.php?mod=VME8011](http://www.caen.it/nuclear/syproduct.php?mod=VME8011;);
724 2008.
- 725 23. Cisco Systems. <http://www.cisco.com/en/US/products/ps6406/index.html>;
726 2011.
- 727 24. Dytman S. LI Summary. MINERvA Doc-DB 4033; 2009.
- 728 25. The CAEN v1720 Waveform Digitizer.
729 <http://www.caen.it/nuclear/product.php?mod=V1720>; 2008.
- 730 26. <http://www.cs.wisc.edu/condor/>; 2011.
- 731 27. <http://www.bira.com/>; 2011.